

Contribution from the Departments of Chemistry, Lanzhou University, Lanzhou, Gansu, PRC, and Northwestern University, Evanston, Illinois 60201

Oxygen Atom Transfer to Metal Carbonyls. Kinetics and Mechanism of CO Substitution Reactions of $M_3(CO)_{11}L$ ($M = Fe, Ru, Os$) in the Presence of $(CH_3)_3NO$

Jian-Kun Shen,[†] Yi-Ci Gao,[†] Qi-Zhen Shi,^{*,†} and Fred Basolo^{*,†}

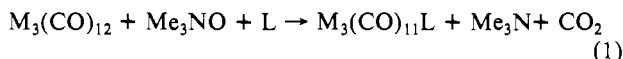
Received May 6, 1988

The rates and activation parameters are reported for CO-substitution reactions of $M_3(CO)_{11}L$ ($M = Fe, L = P(OEt)_3, P(OMe)_3$; $M = Ru, Os, L = P(OEt)_3, P(OMe)_3, P(n-Bu)_3, PPh_3, AsPh_3, SbPh_3$) in the presence of $(CH_3)_3NO$. The rates of reaction are second order, first order in $(CH_3)_3NO$ concentration, first order in $M_3(CO)_{11}L$ concentration, and zero order in entering ligand concentration. For phosphite derivatives, the relative rates are $M_3(CO)_{11}P(OMe)_3 > M_3(CO)_{11}P(OEt)_3$. For other ligand-substituted complexes, the rates of reaction increase with increasing stretching frequency of the CO bands in the IR spectra. The mechanism involved appears to be similar to that proposed earlier of attack by the O atom of $(CH_3)_3NO$ on a C atom of a CO coordinated to an unsubstituted metal atom. The unexpected slow rates for the reactions of $M_3(CO)_{11}P(OR)_3$ are discussed in terms of shorter M-M bond distances in the cluster.

Introduction

The kinetics and mechanisms of thermal substitution reactions of $M_3(CO)_{12}$ ($M = Fe, Ru, Os$) and of corresponding mono- and disubstituted compounds have been studied in some detail.¹ These results show the reactions may involve a variety of mechanisms, including dissociation, association, metal-metal bond cleavage, and cluster fragmentation.

In an attempt to obtain a simple reaction pathway for CO substitution of metal clusters, we recently investigated² the reactions of the $M_3(CO)_{12}$ in the presence of Me_3NO (eq 1). These



reactions take place very rapidly at room temperature in aprotic solvents, but the rates of reaction decrease with added protonic solvent. The reaction rates are first order in concentrations of the cluster and of Me_3NO but zero order in entering ligand and inversely proportional to concentration of added protonic solvent. Under the mild conditions of these reactions, it appears the reactions proceed without complications via the coordinatively unsaturated intermediate $M_3(CO)_{11}$.

Our studies have now been extended to CO substitution reactions of the monosubstituted clusters $M_3(CO)_{11}L$ in the presence of added Me_3NO , in order to determine the electronic and/or steric effect of ligand L on the rates and mechanisms of reaction.

Experimental Section

Compounds and Solvent. $CHCl_3$ was dried with P_2O_5 and distilled prior to use. $M_3(CO)_{12}$ were obtained from the Aldrich Chemical Co. EPh_3 ($E = P, As, Sb$) were purified by recrystallization from anhydrous alcohol. The $P(OR)_3$ compounds were obtained from Merck-Schuchardt. $P(n-Bu)_3$ was provided by the Shanghai Institute of Organic Chemistry. Manipulations involving $Fe_3(CO)_{12}$ or $P(n-Bu)_3$ were routinely carried out under an Ar atmosphere by standard Schlenk techniques. Trimethylamine *N*-oxide was synthesized and purified by the literature method.³

Kinetic Measurements. Infrared spectra were recorded on a Nicolet-5 DX FT IR instrument using a 0.5-mm NaCl cell. All the $M_3(CO)_{11}L$ compounds were studied in situ. The solutions of $M_3(CO)_{11}L$ were prepared² by injecting a solution of $M_3(CO)_{12}$ into a tube containing a solution of L and of Me_3NO . The monosubstitution reaction takes place with mixing, and the slower disubstitution reaction that followed was monitored. The IR spectra had bands at 2100.7 (w), 2046.4 (s), 2011.8 (s) cm^{-1} and 2080.9 (w), 2025.5 (s), 2001.7 (s) cm^{-1} for $Ru_3(CO)_{11}P(OEt)_3$ and $Ru_3(CO)_{10}[P(OEt)_3]_2$, respectively. For $Os_3(CO)_{11}P(OEt)_3$ and $Os_3(CO)_{10}[P(OEt)_3]_2$, IR spectra exhibited bands at 2109.4 (w), 2054.3 (s), 2037.0 (ms), 2019.8 (vs), 1985.3 (ms) cm^{-1} and 2090.8 (w), 2033.2 (ms), 2004.0 (s) cm^{-1} , respectively. Other mono- and disubstituted products obtained under the same condition exhibited IR spectra in good agreement with reported spectra of the known compounds.^{4,5}

Ultraviolet-visible spectral measurements were obtained on a Shimadzu UV-240 spectrophotometer using 1-cm quartz cells. The reactions

Table I. Observed Rate Constants for Reaction 2 in $CHCl_3$ at 17.2 °C and an Me_3NO Concentration of 10.9×10^{-3} M

M	L	$10^3[L], M$	$10^3k_{obsd}, s^{-1}$
Fe	$P(OEt)_3$	5.50	2.67
		11.0	3.04
		16.5	3.12
		22.0	3.09
Ru	PPh_3	3.18	4.94
		6.36	5.18
		9.54	5.10
		12.7	5.05
Os ^a	$AsPh_3$	3.25	9.63
		6.45	9.77
		9.67	9.75
		12.9	9.64

^a At 25 °C and $[Me_3NO] = 4.05 \times 10^{-3}$ M in CH_2Cl_2 .

of $M_3(CO)_{11}L$ with Me_3NO in the presence of L were studied at temperatures between 12 and 36 °C. All reactions were performed under pseudo-first-order conditions with the concentrations of Me_3NO and of ligand being at least 10 times that of $M_3(CO)_{11}L$. Rate data were obtained by monitoring UV-vis spectral changes. In a typical experiment a solution of Me_3NO and a solution of PPh_3 in $CHCl_3$ were mixed in a cuvette, which was then placed in a temperature-regulated jacket. Constant temperature was maintained by the internal circulating bath of the Shimadzu UV-240, which can maintain the reaction temperature to within ± 0.05 °C. After about 30 min of temperature equilibration, a solution of $M_3(CO)_{12}$ in $CHCl_3$ was syringed into the cuvette and the parent compounds were converted into $M_3(CO)_{11}PPh_3$ immediately. The cuvette was removed, vigorously shaken, and then replaced in the light beam, and the resultant spectral changes were monitored by scanning the wavelength range 300-600 nm. No detectable photochemical effect of the light beam was observed by monitoring the reactions at different scan rates.

Plots of $\ln(A_\infty - A_t)$ vs time for appearance of products were linear over 2 half-lives (linear correlation coefficient > 0.999). The slopes of these lines gave values of k_{obsd} .

Results

The rates for the reaction (eq 2) of $M_3(CO)_{11}L$ in $CHCl_3$ solution with entering ligand in the presence of Me_3NO were

$$M_3(CO)_{11}L + Me_3NO + L \rightarrow M_3(CO)_{10}L_2 + Me_3N + CO_2 \quad (2)$$

monitored by following changes in the UV-visible absorption spectra with time. Spectral changes for reaction mixtures show good isosbestic points, in both the UV-visible and the IR regions, suggesting stoichiometric reactions affording disubstituted prod-

- (1) (a) Shojaie, A.; Atwood, J. D. *Organometallics* 1984, 4, 187-190. (b) Poë, A.; Sekhar, V. C. *Inorg. Chem.* 1985, 24, 4376-4380.
- (2) Shen, J. K.; Shi, Y. L.; Gao, Y. C.; Shi, Q. Z.; Basolo, F. J. *Am. Chem. Soc.* 1988, 110, 2414-2418.
- (3) Lecher, H. Z.; Hardy, W. B. *J. Am. Chem. Soc.* 1948, 70, 3789.
- (4) (a) Seamus, M. G.; Marning, A. R. *Inorg. Chim. Acta* 1978, 31, 41-48. (b) Poë, A. J.; et al. *Inorg. Chem.* 1978, 17, 1484. (c) Johnson, B. F. G.; Lewis, J.; Pippard, D. A. *J. Chem. Soc. Dalton Trans.* 1981, 407.
- (5) Bruce, M. I. *Coord. Chem. Rev.* 1987, 76, 1.

[†] Lanzhou University.

[‡] Northwestern University.

Table II. Second-Order Rate Constants and Activation Parameters for Reaction 2 in CHCl_3 ^a

M	L	T, °C	$k_2, \text{M}^{-1} \text{s}^{-1}$	$\Delta H^\ddagger, \text{kcal/mol}$	$\Delta S^\ddagger, \text{cal/(mol-deg)}$
Fe	P(OEt) ₃	12.1	0.132	14.4 ± 0.8	-11.8 ± 2.6
		17.2	0.230		
		24.1	0.389		
		32.1	0.783		
Ru	P(OEt) ₃	12.1	0.116	12.9 ± 0.6	-17.5 ± 2.1
		17.2	0.191		
		24.1	0.328		
		32.1	0.555		
	PPh ₃	12.1	0.252	12.8 ± 0.9	-16.3 ± 3.0
		17.2	0.424		
Os	PPh ₃	17.2	0.0706	16.5 ± 0.2	-7.07 ± 0.63
		25.2	0.152		
		30.6	0.256		
		35.8	0.418		
		35.8	0.418		

^a[P(OEt)₃] = 5.50 × 10⁻³ M; [PPh₃] = 3.18 × 10⁻³ M.

Table III. Second-Order Rate Constants for Reaction 2 in CHCl_3 at 17.2 °C^a

M	L	$k_2, \text{M}^{-1} \text{s}^{-1}$	L	$k_2, \text{M}^{-1} \text{s}^{-1}$
Fe	P(OCH ₃) ₃	0.562	P(OC ₂ H ₅) ₃	0.230
Ru	P(OCH ₃) ₃	0.331	PPh ₃	0.424
	P(OC ₂ H ₅) ₃	0.191	AsPh ₃	0.559
	P(<i>n</i> -Bu) ₃	0.116	SbPh ₃	0.848

^a[PPh₃] = 3.18 × 10⁻³ M; [P(OEt)₃] = 5.50 × 10⁻³ M; [P(*n*-Bu)₃] = 3 × 10⁻³ M; [P(OMe)₃] = 5 × 10⁻³ M; [AsPh₃] = 3 × 10⁻³ M; [SbPh₃] = 5 × 10⁻³ M.

Table IV. Solvent Effects on the Second-Order Rate Constants of Reaction 2 for Os₃(CO)₁₁L

L	T, °C	solvent	$k_2, \text{M}^{-1} \text{s}^{-1}$
P(OCH ₃) ₃	25.2	CHCl ₃	0.104
P(OEt) ₃	25.2	CHCl ₃	0.0609
P(<i>n</i> -Bu) ₃	25.2	CHCl ₃	0.0637
PPh ₃	25.2	CHCl ₃	0.152
AsPh ₃	25.2	CHCl ₃	0.180
SbPh ₃	25.2	CHCl ₃	0.240
PPh ₃	16.6	CH ₂ Cl ₂	0.674
AsPh ₃	16.6	CH ₂ Cl ₂	0.724
P(<i>n</i> -Bu) ₃	16.6	CH ₂ Cl ₂	0.629

ucts. For iron, only two phosphite-substituted complexes, Fe₃(CO)₁₁P(OMe)₃ and Fe₃(CO)₁₁P(OEt)₃, were studied. Unfortunately, P(OPh)₃ is readily oxidized by Me₃NO under the experimental conditions employed. Also trialkylphosphine-disubstituted iron complexes easily fragment, as mentioned earlier by other investigators.^{4a}

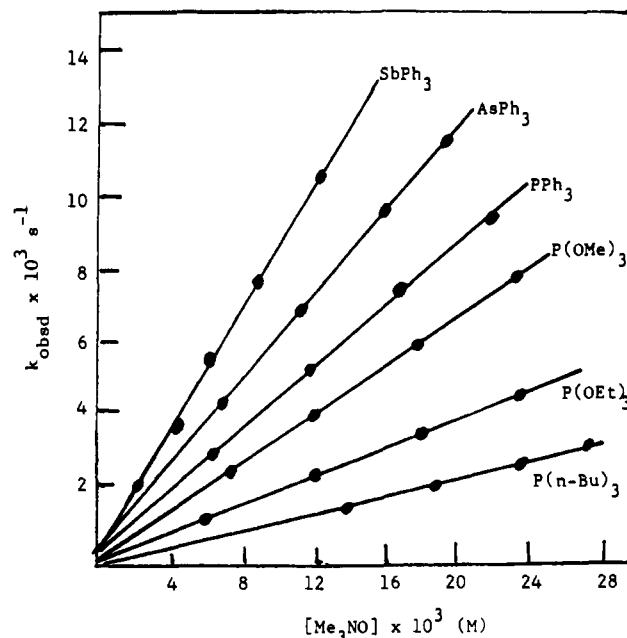
Plots of k_{obsd} vs Me₃NO concentration shown a first-order dependence on trimethylamine *N*-oxide concentration (Figure 1), and the rates of reaction are zero order in entering ligand concentration (Table I). Thus, CO substitution obeys the second-order rate law given by eq 3. Kinetic data for the reaction (eq

$$-\text{d}[\text{M}_3(\text{CO})_{11}\text{L}]/\text{d}t = k_2[\text{M}_3(\text{CO})_{11}\text{L}][\text{Me}_3\text{NO}] \quad (3)$$

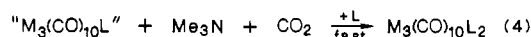
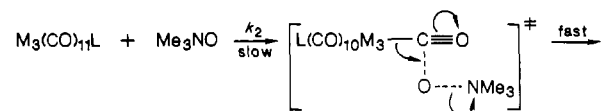
2) are given in Tables II–IV, where values of k_2 have linear correlation coefficients <0.995.

Discussion

Kinetic studies show that the reactions investigated (eq 2) are second order, first order in complex concentration, first order in Me₃NO concentration (Figure 1), and zero order in entering ligand concentration (Table I). This second-order rate law (eq 3) suggests an associative mechanism, as do the low values of ΔH^\ddagger and negative values of ΔS^\ddagger . These results are similar to what was found for the corresponding reactions of M(CO)₆⁶ and of M₃-

**Figure 1.** Plot of k_{obsd} vs Me₃NO concentration for the reaction $\text{Ru}_3(\text{CO})_{11}\text{L} + \text{Me}_3\text{NO} + \text{L} = \text{Ru}_3(\text{CO})_{10}\text{L}_2 + \text{Me}_3\text{N} + \text{CO}_2$ in CHCl_3 at 17.2 °C.

(CO)₁₂² with L in the presence of (CH₃)₃NO. The mechanism suggested earlier^{2,5} could well apply here (eq 4). For that



mechanism, the rate-determining step involves nucleophilic attack of the O atom of Me₃NO on the C atom of a carbonyl group. The presumed transition state then undergoes a redox reaction, forming the good leaving group CO₂ and generating the coordinatively unsaturated intermediate “M₃(CO)₁₀L”. This intermediate readily accepts an entering ligand, forming the disubstituted product M₃(CO)₁₀L₂.

Previous studies^{7,8} have shown that the degree of M→CO π back-bonding influences the reactivity of the C atom of CO toward nucleophilic attack. This same behavior is found for the reactions of M₃(CO)₁₁L with Me₃NO in CHCl₃ solution. The relative degree of M→CO π back-bonding in analogous metal carbonyls is indicated by their CO stretching frequencies, where the lower the frequency the greater the degree of back bonding. This transfer of electron density from metal atom to CO makes the C atom of the carbonyl group less positive and thus less susceptible to nucleophilic attack. As shown in Figure 2, the rates of reaction for phosphine-type ligand derivatives of the cluster increase with increase in frequency of the highest energy ν_{CO} of the complexes. However, this does not apply to the corresponding phosphite derivatives, which react much more slowly than expected on the basis of their ν_{CO}. This point is addressed later, but one other thing to note is that M₃(CO)₁₁P(OEt)₃ reacts more slowly than does M₃(CO)₁₁P(OMe)₃ (Tables III and IV), although the compounds have about the same values of ν_{CO}. This difference in rate may reflect the slightly greater proton basicity⁹ of P(OEt)₃ vs that of P(OMe)₃, which in turn results in the C atoms of the CO's of the P(OEt)₃ cluster being less positive and less susceptible to nucleophilic attack than is the P(OMe)₃ cluster.

(6) Shi, Y. L.; Gao, Y. C.; Shi, Q. Z.; Basolo, F. *Organometallics* **1987**, *6*, 1528.

(7) Darensbourg, M. Y.; Condor, H. L.; Darensbourg, D. J.; Hosday, C. *J. Am. Chem. Soc.* **1973**, *95*, 5919–5924.

(8) Gao, Y. C.; Shi, Q. Z.; Kershner, D. L.; Basolo, F. *Inorg. Chem.* **1988**, *27*, 188.

(9) Rahman, M.; Liv, H. Y.; Prock, A.; Giering, W. P. *Organometallics* **1987**, *6*, 650–658.

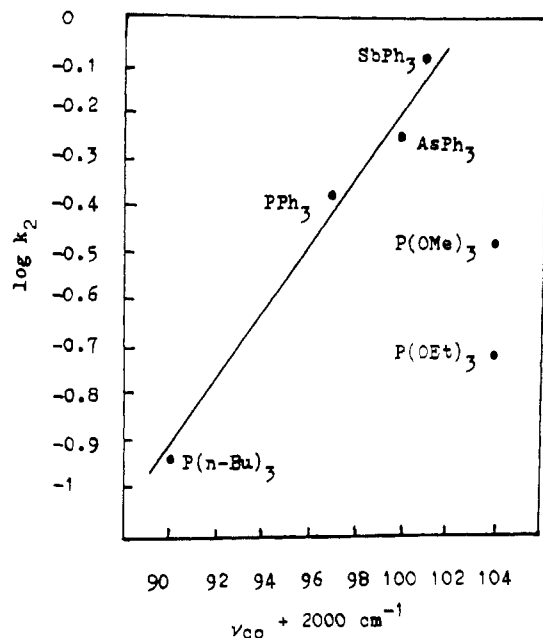


Figure 2. Plot of $\log k_2$ vs ν_{CO} for the reaction $\text{Ru}_3(\text{CO})_{11}\text{L} + \text{Me}_3\text{NO} + \text{L} = \text{Ru}_3(\text{CO})_{10}\text{L}_2 + \text{Me}_3\text{N} + \text{CO}_2$ in CHCl_3 at 17.2°C .

Table V. Rate Constants (k_2 , $\text{M}^{-1} \text{s}^{-1}$) for the Oxygen Atom Transfer Reactions of $\text{M}_3(\text{CO})_{11}\text{L}$ Clusters in CHCl_3 at 4.5°C

L	M = Fe	M = Ru	M = Os
CO	47.1 ^a	8.50	0.784
PPh_3		0.140	0.0180
P(OEt)_3	0.0676	0.0640	

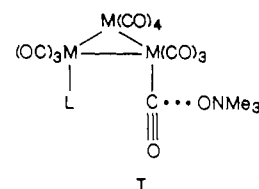
^a Estimated from data in ref 2.

The same qualitative correlation of rate to ν_{CO} was observed for the reactions of $\text{Os}_3(\text{CO})_{11}\text{L}$ with Me_3NO (Table IV) in CHCl_3 , although the rate variations are smaller than for the Fe and Ru clusters. It is further of interest that the clusters $\text{Os}_3(\text{CO})_{11}\text{L}$ ($\text{L} = \text{PPh}_3, \text{AsPh}_3, \text{P}(n\text{-Bu})_3$) react with Me_3NO at about the same rate in CH_2Cl_2 . This suggests that neither the electronic nor the steric properties of L have a large effect on the rates of reaction in CH_2Cl_2 . The reason for this difference of rate behavior between the two solvents is not clear, but it may reflect the greater hydrogen bonding of Me_3NO in CHCl_3 than in CH_2Cl_2 ($\text{Me}_3\text{NO} \cdots \text{HCCl}_3$). In such a case, Me_3NO is freer to react in CH_2Cl_2 and less discriminating in its rates of reaction than when more solvated in CHCl_3 . Consistent with this is the fact that reactions in CH_2Cl_2 are faster than in CHCl_3 .

Rates of the reactions of $\text{M}_3(\text{CO})_{11}\text{L}$ (eq 2) are less than those for the corresponding reactions of $\text{M}_3(\text{CO})_{12}$ (Table V). This is as expected because the positive charge on the carbonyl carbon is less on the substituted cluster than on the parent cluster and because the more positive the carbonyl carbon the more susceptible it is to nucleophilic attack. Support of the charge on the carbonyl carbon is provided by the lower values of ν_{CO} for the substituted cluster relative to the parent, indicating more electron density in $\text{M}_3(\text{CO})_{11}\text{L}$ and more metal to carbonyl back bonding than in $\text{M}_3(\text{CO})_{12}$. It is further of interest to note that this retardation of reaction rate for substituted clusters is just the opposite to what was found for associative thermal CO substitution reactions.^{1b} The accelerated thermal rate for substituted clusters was attributed to their longer metal-metal bonds relative to that of the parent, this then allowing a more favorable attack by the entering nucleophile on the metal atom.

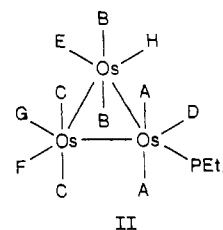
The additional electron density introduced into the cluster by replacing a CO with L is believed to be distributed throughout the cluster. However, the inductive effect of L is expected to be larger on the carbonyls coordinated to the same metal atom as is L than it is on the carbonyls coordinated to the other two metal atoms. In such a case, the carbonyls on the other two metal atoms would have a greater positive charge on carbon and would then

be the sites of attack by Me_3NO (see structure I). The IR spectra

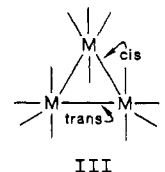


of the $\text{M}_3(\text{CO})_{10}\text{L}_2$ products obtained show that the two ligands are on different metal atoms, in agreement with known X-ray-determined structures of such clusters.⁵

That the two ligands are situated on different metals is further supported by the ^{13}C NMR chemical shifts for $\text{M}_3(\text{CO})_{11}\text{L}$. As shown in structure II, the spectrum of $\text{Os}_3(\text{CO})_{11}\text{PEt}_3$ at -60°C



shows eight resonances, viz. (A) 194.1, (C) 186.3, (B) 184.4, (H) 178.1, (D) 176.8, (E) 173.8, (F) 172.8, and (G) 170.4 ppm.¹⁰ Compared with the $\delta(^{13}\text{C})$ values of $\text{Os}_3(\text{CO})_{12}$ (two resonances at 182.5 and 170.4 ppm), those of $\text{Os}_3(\text{CO})_{11}\text{PEt}_3$ are shifted to lower field due to paramagnetic effects caused by an increase in the $\text{M} \rightarrow \text{CO}$ back-bonding interaction.¹² As more electron density is returned to CO by back-bonding, the $\delta(^{13}\text{C})$ values increase and the ν_{CO} values decrease (see above). Since the $\delta(^{13}\text{C})$ values of ^{13}C on the two unsubstituted Os atoms are less than the corresponding ^{13}C values on the substituted Os atom, the C atoms of the former kinds of carbonyls are expected to be more susceptible to nucleophilic attack than that of the latter. Furthermore, it was found⁵ that phosphorus-containing ligands always occupy the equatorial position in $\text{M}_3(\text{CO})_{11}\text{L}$, and the $\text{M}-\text{M}$ bond cis to L is longer than the one trans to L (see structure III). Therefore,



the C atoms of carbonyls on the cis-Os atom are more positive and the most reactive toward nucleophilic attack among all the C atoms of the cluster. In support of this is our study⁸ on the same reaction of $\text{Mo}(\text{CO})_5\text{L}$ that showed that the nucleophilic attack of Me_3NO is on the C atom cis to L, which has a lower $\delta(^{13}\text{C})$ value than does the CO trans to L.

The P(OEt)_3 - and P(OMe)_3 -substituted complexes are less reactive than expected on the basis of their ν_{CO} values. The two ligands have smaller cone angles¹³ than the other ligands studied. Crystal structure analysis⁵ showed that the $\text{Os}-\text{Os}$ bonds between L-substituted Os and unsubstituted Os atoms are longer in $\text{Os}_3(\text{CO})_{11}\text{PPh}_3$ (cis 2.918, trans 2.891, other 2.886 Å) than in $\text{Os}_3(\text{CO})_{11}\text{P(OMe)}_3$ (cis 2.908, trans 2.890, other 2.892 Å). Although $\text{M}-\text{M}$ bonds in $\text{Ru}_3(\text{CO})_{11}\text{P(OMe)}_3$ are unknown, the analogous complex $\text{Ru}_3(\text{CO})_{11}\text{PPh(OEt)}_2$ (cis 2.872, trans 2.846, other 2.858 Å) does have a shorter $\text{Ru}-\text{Ru}$ bond than does $\text{Ru}_3(\text{CO})_{11}\text{PPh}_3$ (cis 2.907, trans 2.876, other 2.875 Å). The shorter $\text{M}-\text{M}$ bond may enhance the inductive effect of L on the CO's of neighboring metals and lessen their reactivity toward

(10) Johnson, B. G. F.; Lewis, J.; Bernhard, E. R.; Karl, T. S. *J. Chem. Soc., Dalton Trans.* **1976**, 1403.

(11) Lewis, L.; Johnston, B. G. F. *P. A. Chem.* **1975**, *44*, 43.

(12) Bodner, G. M.; May, M. P.; McKinney, L. E. *Inorg. Chem.* **1980**, *19*, 1951-1958.

(13) Tolman, C. A. *Chem. Rev.* **1977**, *77*, 313.

Me_3NO in accord with the observation that phosphite derivatives of metal carbonyl clusters react more slowly than expected relative to corresponding phosphine-type derivatives.

The differences in rates of reaction between $\text{M}_3(\text{CO})_{12}$ and $\text{M}_3(\text{CO})_{11}\text{L}$ for a given metal decrease in the order $\text{Fe} > \text{Ru} > \text{Os}$ (Table V). This too can be explained in terms of the M–M bond length order of $\text{Fe–Fe} < \text{Ru–Ru} < \text{Os–Os}$,⁵ which in turn mirrors the decreasing order of the inductive effect of L and thus the rates of reaction of $\text{M}_3(\text{CO})_{11}\text{L}$. The complex $\text{Fe}_3(\text{CO})_{11}\text{L}$ has two bridging carbonyls,⁵ which may also enhance the effect of L on the reactivity of the CO groups. It is of interest to note that the difference in the rates of reaction between $\text{Fe}_3(\text{CO})_{12}$ and

$\text{Fe}_3(\text{CO})_{11}\text{L}$ is as large as that between $\text{M}(\text{CO})_6$ and $\text{M}(\text{CO})_5\text{L}$,⁸ where the nucleophilic attack on the monomeric metal carbonyls has to be on a CO coordinated to the same metal atom as L.

Acknowledgment. We wish to thank the United States-China Cooperative Science Program for the support of this collaborative research. The program is supported by the U.S. National Science Foundation and the PRC National Natural Science Foundation.

Supplementary Material Available: Table with additional rate data for the reactions under study (eq 2) and figures of IR and UV–vis absorbance changes versus reaction time (10 pages). Ordering information is given on any current masthead page.

Contribution from the Department of Chemistry and The Quantum Theory Project, University of Florida, Gainesville, Florida 32611

Electronic Causes of Dissymmetry in Side-On-Bonded Dioxxygen Complexes

Thomas R. Cundari, M. C. Zerner,* and R. S. Drago*

Received December 21, 1987

The underlying reasons for the distortion of transition-metal tetraperoxides $\text{M}[\text{O}_2]_4^{n-}$ ($\text{M} = \text{Cr}$, $n = 3$; $\text{M} = \text{Mo}$, $n = 2$) are investigated. INDO/1 calculations are used. The method employed is to start with the symmetrical coordination mode (i.e. equal M–O bond lengths) and to look for significant differences in specific orbital interactions, which lead to the observed asymmetric geometry. Gradient optimization confirms the observation. The distortion is due to the greater interaction of the oxygen 2s orbitals (axial > equatorial) with the transition-metal p_x orbital. This interaction is made energetically feasible due to the high oxidation state of the metal and the negative charge on the peroxide fragment.

Introduction

Transition-metal peroxides are an important class of compounds in the oxidation of various organic substrates.^{1,2} In particular, η^2 -dioxxygen complexes of group VIB metals have been used for epoxidations.^{3,4} Theoretical investigations of this reaction have been reported.⁵ In a number of these systems there exist small deviations of the dioxxygen ligand from a symmetrical, isosceles triangle geometry.⁶ This present research has sought electronic reasons for this dissymmetry in the particular case of metal tetraperoxides.

Since any mechanism of transition-metal η^2 -peroxide catalyzed epoxidation^{7,8} must involve the breaking of a metal–oxygen bond, differences in their strengths will have important implications in both the Sharpless⁸ and Mimoun mechanisms.⁷

We have focused our attention on $\text{Mo}[\text{O}_2]_4^{2-}$ and $\text{Cr}[\text{O}_2]_4^{3-}$, which due to their reasonable size, high symmetry and large distortion from symmetrical coordination are ideal for this investigation (Figure 1). While there have been theoretical investigations^{9–14} into the bonding of peroxides to metals, the reasons

Table I. Geometrical Parameters^{a, b}

metal	$r(\text{M–Oe})$	$r(\text{M–Oa})$	$r(\text{Oa–Oe})$	$\angle(\text{Oe–M–Oe}')$	$\angle(\text{Oe–M–Oa})$
Cr	1.958	1.882	1.466	175.37	44.83
Mo(obs)	2.000	1.930	1.546	177.20	46.30
Mo(calc)	1.97	1.92	1.24	179.4	37.0

^a Taken from ref 9. ^b Distances in angstroms; angles in degrees.

for the observed difference in metal–oxygen bond lengths in these complexes has never been fully addressed.

Calculations

The INDO/1 semiempirical method was used.^{15,16} Chromium tetraperoxide is an open-shell molecule, so the unrestricted Hartree–Fock formalism was used.¹⁷ For molybdenum tetraperoxide a restricted wave function was used. Two sets of calculations were run on each molecule—at the experimentally determined geometries, given in Table I, and at a symmetrical geometry in which all the M–O bond lengths are equal to each other and the average of the observed bond length. Any important bonding interactions will be present in both. The bond order, overlap, Fock matrix elements, and atomic bond index are similar in both the symmetric and asymmetric geometries since the distortion is slight. The symmetrical configuration was studied in depth, and electronic causes for the geometric perturbation were investigated.

For two atomic orbitals to interact,¹⁸ (1) they must overlap and (2) they must be of similar energy. A difference in the metal–oxygen in-

- Gubelmann, M. H.; Williams, A. F. *Structure and Bonding*; Springer-Verlag: Berlin, 1983; Vol. 55.
- Lyons, J. E. In *Aspects of Homogeneous Catalysis*; Ugo, R., Ed.; Reidel: Dordrecht, The Netherlands, 1977; Vol. 3.
- Mimoun, H. In *Comprehensive Inorganic Chemistry*, in press.
- Winter, W.; Mark, C.; Schurig, V. *Inorg. Chem.* **1980**, *19*, 2043.
- (a) Jørgensen, K. A.; Wheeler, R. A.; Hoffmann, R. *J. Am. Chem. Soc.* **1987**, *109*, 3240. (b) Jørgensen, K. A.; Hoffmann, R. *Acta Chem. Scand.* **1986**, *B40*, 411. (c) Purcell, K. *Organometallics* **1985**, *4*, 509.
- (a) Halpern, J. A.; Goodall, B. A.; Khare, J. P.; Lim, H. S.; Pluth, J. *J. Am. Chem. Soc.* **1975**, *97*, 2301. (b) Terry, N. W.; Amma, E. L.; Vaska, L. *J. Am. Chem. Soc.* **1972**, *94*, 653.
- Mimoun, H.; Seree de Roch, I.; Sajus, L. *Tetrahedron* **1970**, *26*, 37.
- Sharpless, K. B.; Townsend, J. M.; Williams, D. R. *J. Am. Chem. Soc.* **1972**, *94*, 295.
- Roch, M.; Weber, J.; Williams, A. F. *Inorg. Chem.* **1984**, *23*, 4571.
- Brown, D. H.; Perkins, R. H. *Inorg. Chim. Acta* **1974**, *8*, 285.
- Dacre, P. D.; Elder, M. *J. Chem. Soc., Dalton Trans.* **1972**, 1426.

- Fischer, J.; Veillard, A.; Weiss, R. *Theor. Chim. Acta* **1972**, *24*, 317.
- Rosch, N.; Hoffmann, R. *Inorg. Chem.* **1974**, *13*, 2656.
- Swalen, J. D.; Ibers, J. A. *J. Chem. Phys.* **1962**, *37*, 17.
- (a) Bacon, A. D.; Zerner, M. C. *Theor. Chim. Acta* **1979**, *53*, 21. (b) Andersen, W.; Edwards, W. D.; Zerner, M. C. *Inorg. Chem.* **1986**, *25*, 2728.
- Pople, J. A.; Beveridge, D. L. *Approximate Molecular Orbital Theory*; McGraw-Hill: New York, 1970.
- Pople, J. A.; Nesbet, R. K. *J. Chem. Phys.* **1954**, *22*, 571.
- (a) Whangbo, M.-H.; Burdett, J.; Albright, T. *Orbital Interactions in Chemistry*; Wiley: New York, 1970. (b) Whangbo, M.-H.; Schlegel, H. B.; Wolfe, S. *J. Am. Chem. Soc.* **1977**, *99*, 1296.